

Preparation and Performance of Filled Resin Based on Long Afterglow Materials in Gingival Wall Lifting Surgery

Yijun ZOU, Yine MEI, Yuling PANG *

Department of Stomatology, Wuhan Dongxihu District People's Hospital, Wuhan 430040, Hubei, China

<http://doi.org/10.5755/j02.ms.38204>

Received 24 July 2024; accepted 14 November 2024

The study was conducted to solve the problems of low monomer conversion rate and insufficient curing depth of dental resin complexes during curing in gingival wall elevation procedures. A dental composite resin was prepared by modifying the blue emitting long afterglow luminescent material. Then it was applied in the treatment of oral caries for experimental research. The results showed that the afterglow of the SMSSED material showed high brightness and blue, with its thermoluminescence peak higher than that of the control group, reaching a maximum of 3×10^6 . The curing performance was better. It was 9.17 % higher than CAED and 10.27 % higher than SAED. The accuracy of the measurements for the different resins in the study was about 5.67 %. In addition, the double bond conversion rate of the composite resin doped with 1 wt.% increased by 114.16 % compared to the composite resin without SMSSED doping. The structure and size of composite resins containing 1 wt.% research materials were more stable. Overall, the cell survival rate for 1–3 days was higher than 70 %, indicating that the modified composite resin had lower toxicity to L929 cells. Overall, the performance of the dental composite resin prepared by modifying the blue emitting long afterglow luminescent material is significantly improved, indicating its effectiveness and practicality. It can be practically applied in the treatment of dental caries in gingival wall lifting surgery.

Keywords: gingival wall lifting surgery, long afterglow materials, filling resin, caries, toxicity.

1. INTRODUCTION

Caries is a chronic, progressive disease that damages the hard tissue of teeth due to bacteria and various other reasons. It is commonly referred to as "tooth decay", which is manifested as the demineralization of inorganic substances and decomposition of organic substances [1–3]. Although the improvement in economic level has significantly improved the treatment rate of dental caries, the incidence rate remains high. Gingival wall lifting surgery, as a new method to replace crown elongation surgery, can effectively solve a series of adhesive repair problems such as deep adjacent defects, enamel loss, and difficulty in moisture isolation [4–6]. In gingival wall elevation surgery, dental filling techniques are commonly used in clinical practice to treat caries and repair damaged teeth. Traditional filling materials such as amalgam and glass ionomer cement have biological safety issues. It is difficult to achieve the matching degree and high mechanical strength between composite resin and tooth color [7, 8]. Dental Resin Composite (DRCs), as a new type of material, has significant advantages. Compared to silver amalgam, it has higher biological safety, higher mechanical properties, and longer lifespan. Therefore, it has become the most suitable filling and repairing material in clinical practice [9, 10]. However, current DRCs may exhibit edge gaps and defects during the filling process, promoting micro leakage and leading to secondary caries. At the same time, participating in stress will gradually form, thereby reducing the biocompatibility, durability, and mechanical properties of the oral composite resin [11, 12]. The modification

methods for DRCs are prone to lower double bond conversion rates and lower viscosity. In some cases, there may be a higher risk of local toxicity. Long afterglow luminescent materials are a typical type of photoluminescence material. Due to its excellent luminescence and afterglow performance, it has a wide range of applications in photocatalytic degradation, photodynamic therapy, and other fields. In dentistry, the laser wavelength of some long afterglow materials is also within the working range of the curing lamp [13]. Therefore, based on nanomaterials, the dental composite resin is modified and prepared using the blue emitting long afterglow luminescent materials ($\text{Sr}_2\text{MgSi}_2\text{O}_7: \text{Eu}^{2+}, \text{Dy}^{3+}$; SMSSED). Its purpose is to solve the low monomer conversion rate and insufficient curing depth of current DRCs, providing theoretical references for the application of long afterglow materials in dentistry. At the same time, there is currently some research on long afterglow materials in cancer treatment and emergency lighting. There is relatively little research on the application of dental caries treatment in dentistry. The research on the modification of dental composite resin is also relatively insufficient. Therefore, the SMSSED modification for preparing dental composite resins is innovative.

2. MATERIALS AND METHODS

2.1. Reagents

The reagents used in this study were purchased from commercial suppliers. Blue purple long afterglow

* Corresponding author: Y. Pang
E-mail: pangyuling@wddph.ac.cn

luminescent materials (CaAl_2O_4 : Eu^{2+} , Dy^{3+} , CAED), blue green long afterglow luminescent materials ($\text{Sr}_4\text{Al}_{14}\text{O}_{25}$: Eu^{2+} , Dy^{3+} , SAED), and SMSSED were provided by Foshan Ruiying New Materials Co., Ltd. Bisphenol A glycerol dimethyl acrylate (99 %), ethyl 4-(N, N-dimethylamino) benzoate (99 %), camphorquinone (97 %), and triethylene glycol dimethacrylate (99 %) were purchased from Sigma-Aldrich. KH570-nano SiO_2 was sourced from Hebei Yonghua Wear-resistant Materials Co., Ltd., and anhydrous ethanol (A.R.) was obtained from Tianjin Chemical Reagent Co., Ltd. Hexane (99 %) was purchased from Shanghai Aladdin Biochemical Technology Co., Ltd., while polyester film forming sheets (100 pieces) were provided by Guilin Botong Trading Co., Ltd. DMEM high sugar culture medium (500 mL), trypsin (1:250) (100 g), horse serum (200 mL), and penicillin-streptomycin solution (100 mL) were obtained from Gibco and Solarbio, respectively. The Cell Counting Kit was sourced from Abmole Bioscience, and the LIVE/DEAD™ Cell Imaging Kit was provided by Invitrogen. All chemicals and reagents were used as received without further purification unless otherwise stated.

2.2. Instruments

The experiments were carried out using various instruments including an electronic balance (Sartorius BP221S, Sadolis Beijing AG, Germany), an agate mortar (14 cm, Jinzhou Yuxiangyuan Agate Products Factory, China), and a heating and drying oven (DHG Series DZF-6020, Shanghai Yiheng Scientific Instrument Co., Ltd., China). A digital temperature control magnetic stirrer (SZCL-2, Shanghai Sile Instrument Co., Ltd., China) was used for stirring, while an X-ray diffractometer (XRD-6100, SHIMADZU Corporation, Japan) and a field emission scanning electron microscope (JEOLISM-6701F, Nippon Electronic Optics Co., Ltd., Japan) were employed for material characterization. A fluorescence spectrometer (Omni- λ 300i, Beijing Zhuolianguang Instrument Co., Ltd., China) and an afterglow tester (PR305, Zhejiang Sanse Instrument Co., Ltd., China) were used for optical measurements. Additional equipment included a TPC wireless curing lamp (LED55, Dongguan Ligang Medical Equipment Co., Ltd., China), an electronic digital caliper (150 mm, Shanghai Mairuisi International Trade Co., Ltd., China), and a Fourier transform infrared spectrometer (VERTEX 70v, Brucker GmbH, Germany). Mechanical testing was performed using a universal testing machine (AGS-X 500 N, SHIMADZU Corporation, Japan), while a carbon dioxide incubator (IN E800749L, Mert, Germany) and a biosafety cabinet (HFsafe-1200A2, Shanghai Likang Disinfection High Tech Co., Ltd., China) were used for cell culture and biosafety applications. Other equipment included a general refrigerator (HYC-940, Qingdao Haier Co., Ltd., China), a centrifuge (CTK80, Hunan Xiangyi Laboratory Instrument Development Co., Ltd., China), a microplate reader (iMARK, BoLe Company, USA), an inverted phase contrast microscope (IX-71, Olympus Corporation, Japan), an adjustable single channel pipette (Pipet-Lite XLS+, Mettler Toledo Corporation, USA), and a research grade upright fluorescence microscope (NiE, Nikon Corporation, Japan).

2.3. Preparation of modified dental composite resin based on SMSSED

The gingival wall elevation surgery is performed within the biological width range. In the experiment, patients are divided into three groups, namely Group A, Group B and Group C. Group A is treated with SMSSED modified dental composite resin material, Group B is treated with CAED modified dental composite resin material, and Group C is treated with SAED modified dental composite resin material. The traditional oral composite resin used in gingival wall lifting surgery gradually weakens the light transmittance with increasing thickness, while the long afterglow luminescent material can significantly absorb visible light and store it. Therefore, this study uses SMSSED to modify and prepare the dental composite resin. The research mainly explores whether its luminescent properties match the wavelength required by DRCs.

In the experiment, X-ray diffraction (XRD) is used for phase analysis of long afterglow materials and surface KH570 nano SiO_2 (KH570 NS) of nano silica. Excitation source is 1.54178 Å Cu K_α radiation. The working voltage is set to 40 kV and 60 mA. Collect room temperature 2θ is $10^\circ - 80^\circ$. The scanning step size and scanning rate are 0.02 and $15^\circ/\text{min}$. In Scanning Electron Microscope (SEM) analysis, the sample is first dipped in a small amount of conductive adhesive. The powder that has not been adhered to the conductive adhesive is gently blown off with an ear wash ball to avoid interference with the SEM equipment caused by negative pressure pollution, which may affect the experimental results. Secondly, the surface morphology of the sample is analyzed using SEM with a voltage of 10 kV as the observation voltage. Comparison of the cases of different long afterglow material compositions enables the exploration of the suitability of long afterglow luminescent materials for modification of dental composite resins and whether the luminescent properties of these materials are compatible with the curing requirements of dental resins.

In the preparation of modified light-curing resins, bisphenol A dimethylglycidyl methacrylate and triethyleneglycol dimethacrylate were mixed in a mass ratio of 1:1, and 0.5 % camphor quinone and 0.5 % ethyl 4-N(N-dimethylamino)benzoate were added as photoinitiators for the study. The luminescent powder was mixed with different ratios of KH570-NS, treated with anhydrous ethanol and dried. The resin matrix and filler were mixed and used for depth of cure test. The solidification depth is shown in Eq. 1.

$$GH = L/2, \quad (1)$$

where GH represents the curing depth; L represents the length.

For the curing depth test, the resin was loaded into a 4 mm diameter and 15 mm thick mould and cured for 20 seconds with a photosensitive lamp of wavelength 400–490 nm. The depth of cure was measured by electronic calipers. Photoluminescence spectroscopy was analysed using a 500 W Xe 900 lamp with a wavelength of 200–900 nm, a slit width of 2 mm, and a scanning speed of 240 nm/min. The samples were irradiated with a 365 nm UV lamp for 10 min, and the afterglow decay was monitored. Thermoluminescence (TL) curves were

measured by a FJ427A1 TL dosimeter in a dark room at a test temperature of 250 °C and a heating rate of 1 °C/s.

2.4. Testing of modified composite resin materials

Based on preparing modified dental composite resin with SMSSED, to further verify whether SMSSED is suitable for composite resin, various properties of modified dental composite resin are verified through research. The experimental content includes XRD analysis of composite resin (the experimental method is the same as the composite resin testing), Fourier Transform Infrared Spectroscopy (FTIR) analysis, and scanning electron microscopy analysis of the composite resin fracture surface, composite resin double bond conversion rate, mechanical properties, water absorption rate, solubility, and in vitro biocompatibility testing.

Among them, in FTIR analysis, the powder of KH570-NS and SMSSED samples is crushed and then made into thin sheets using a tablet press. Each composite resin paste is placed in a mold with a diameter of 4 mm and a height of 2 mm. After 20 seconds of illumination, it is taken out and immediately characterized and identified using total reflection FTIR.

SEM is used to observe the particle size, morphology, and filler distribution of samples dried and stored for 24 hours in the analysis of composite resin fracture surfaces. A uniform layer of gold is coated on the fracture morphology of the specimen to reduce electron charge. The fracture morphology is observed.

By sharing the experimental reagents and instrumentation for the effect of long afterglow luminescent materials on the properties of composite resins, the study was able to verify the suitability of SMSSED-modified composite resins for dental restorations, including their biocompatibility, mechanical properties and chemical stability.

When testing the double bond conversion rate of modified composite resin, ATR-FTIR technology was used to measure the double bond conversion rate in the range of 4000 to 400 cm⁻¹. The uncured resin is filled into the mold, and its infrared absorption spectrum is scanned by an ATR crystal. Then, it is irradiated with a curing lamp for 20 seconds and the spectrum is scanned again. Use software to analyze the absorption peak height and calculate the double bond conversion rate, as shown in Eq. 2.

$$D = \left[1 - \left(F_{1636} / F_{1720} \right)_{\text{cured}} / \left(F_{1636} / F_{1720} \right)_{\text{uncured}} \right] \times 100\% \quad (2)$$

where D represents the double bond conversion rate; $(F_{1636} / F_{1720})_{\text{uncured}}$ and $(F_{1636} / F_{1720})_{\text{cured}}$ represent the ratio of absorption peak heights at 1636 cm⁻¹ and 1720 cm⁻¹. For the mechanical performance testing of materials, including elastic modulus (EM) and compressive strength (CS), samples of specific sizes are made and subjected to ultraviolet curing treatment, and then tested using a universal testing machine, as shown in Eq. 3 and Eq. 4:

$$E = (Z\alpha^3) / (4ach^3) \quad (3)$$

where E represents the elastic modulus; Z represents the maximum load; α represents the span of the bracket, which

is 20 mm in the experiment; a represents the width of the sample; c represents the deflection corresponding to E ; h represents the height of the specimen.

$$P = (4R) / (\pi r^2) \quad (4)$$

where P represents the compressive strength; R represents the actual maximum load at the fracture; r represents the radius of the specimen. When testing the water absorption and solubility of materials, the sample is cured in a PTFE mold, dried and soaked, and the water absorption and solubility are calculated by weighing changes, as shown in Eq. 5 and Eq. 6.

$$W = \frac{(m_2 - m_3)}{m_3 V} \times 100\% \quad (5)$$

where W represents the water absorption rate of the material; m_2 represents the quality of discolored silicone gel soaked and drained with filter paper without any moisture; m_3 represents the quality of discolored silicone after being placed in a vacuum dryer; V represents the volume of the specimen.

$$T = \frac{(m_1 - m_3)}{m_1 V} \times 100\% \quad (6)$$

where T represents the solubility of the material; m_1 represents the constant mass of discolored silicone gel that has been dried and replaced in the oven. The in vitro biocompatibility testing of composite resins refers to existing research, mainly including sterilization and extraction, Cell Counting Kit-8 (CCK-8) experiments, and live and dead cell staining experiments [14].

3. RESULTS AND DISCUSSION

3.1. Characterization and performance analysis of modified dental composite resins

To verify the performance of SMSSED modified composite resin materials, experiments are conducted to verify them. Modified materials are mainly used in gingival wall lifting surgery. Therefore, an analysis is conducted on 80 patients who underwent gingival wall elevation surgery at a certain hospital's dental department from November 2022 to December 2023. Among them, there are 48 males and 32 females, aged 18–58 years old. There are a total of 80 teeth, including 43 molars and 37 premolars. All affected teeth have decayed to the subgingival region. Among them, the XRD spectra of KH570-NS and three groups are shown in Fig. 1. From Fig. 1 a, a broad and strong peak appeared when 2θ is around 22.0°, indicating that the NS at this time is in an amorphous form. From Fig. 1 b, all diffraction peaks in the XRD pattern of Group A were consistent with PDF:53-1091. There were no impurity peaks. The XRD pattern of Group B also revealed diffraction peaks of other impurity phases, which was the same as the PDF:75-1736. The XRD pattern of Group C was consistent with PDF:52-1876. Overall, the fit degree of Group A is higher than that of Group B and Group C. The performance is relatively better.

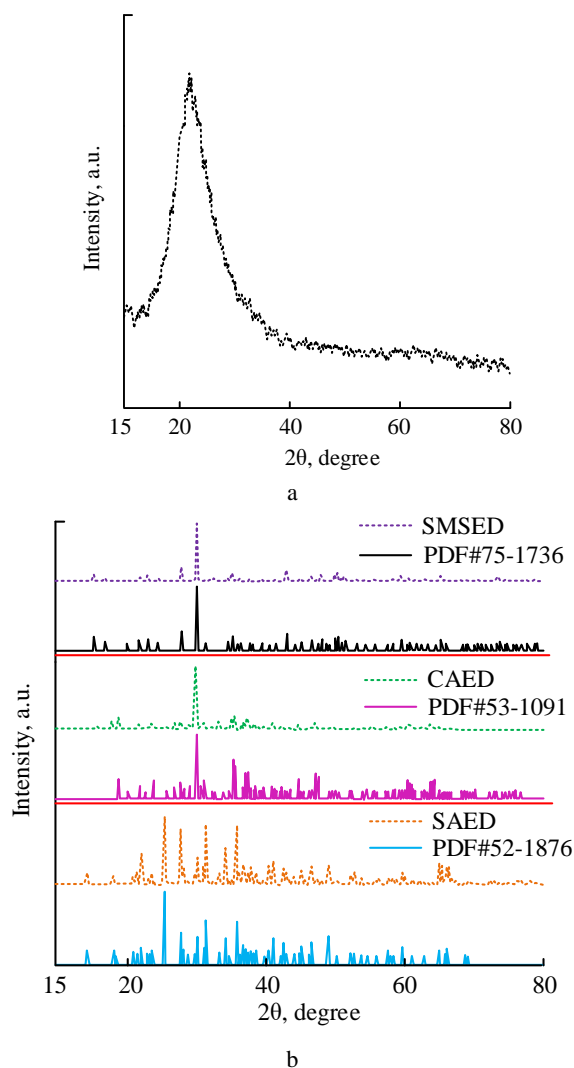


Fig. 1. a–XRD pattern of KH570-NS; b–XRD patterns of SMSSED, CAED, and SAED

The SEM images of KH57-NS and three groups are shown in Fig. 2.

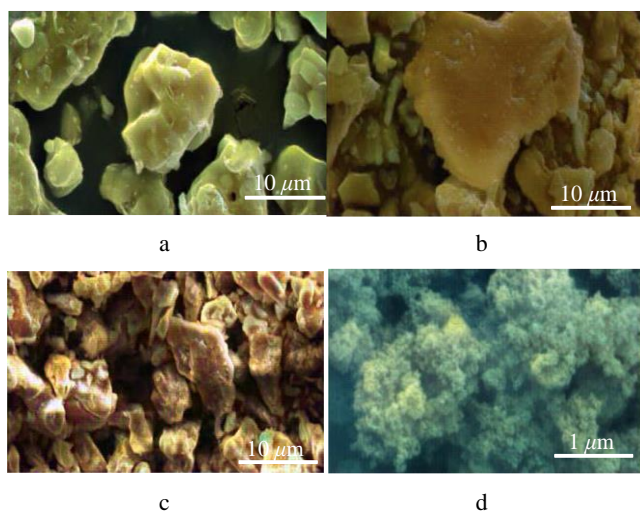


Fig. 2. a–SEM images of KH570-NS; b–SEM images of SMSSED; c–SEM images of CAED; d–SEM images of SAED

From Fig. 2 a, the diameter of KH570-NS particles was around 20 nm. There was a significant aggregation phenomenon and irregular particle shape. From Fig. 2 b, c, and d, compared to the surface morphology results of Group B and Group C, the powder of Group A presented a blocky agglomeration state, with a huge size distribution and irregular shape. This result is closer to the relevant particle size distribution of commercial strontium aluminate phosphors. In addition, the results of three sets of excitation emission spectra, afterglow attenuation curves and afterglow images, and TL spectra are shown in Fig. 3.

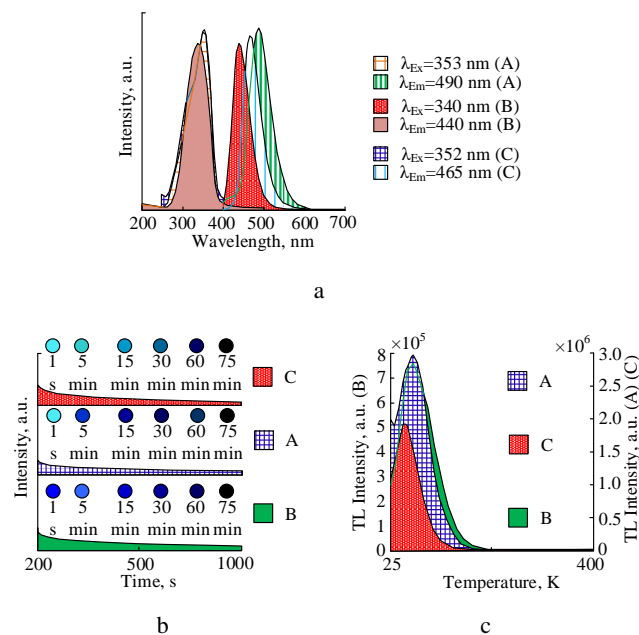


Fig. 3. a – three sets of excitation emission spectra; b – three sets of afterglow attenuation curves and afterglow images; c – three sets of thermoluminescence spectra

From Fig. 3 a, the excitation spectrum of Group A exhibited a broadband of 260–400 nm. The maximum excitation wavelength was 352 nm. The emission spectrum had a broad peak emission of 490 nm. From Fig. 3 b, the afterglow of SMSSED displayed high brightness and blue. After removing the light source, the afterglow experienced two stages: rapid decay and prolonged duration. From Fig. 3 c, all three materials had relatively shallow trap depths. Room temperature environment excited electrons stored in trap energy levels, thereby producing growth afterglow luminescence. The TL peak of Group A was higher than that of the control group, reaching the highest value 3×10^6 .

Finally, the Cured Depth (CD) values of the three modified composite resins are compared. The results are shown in Table 1. From Table 1, when the actual content of the three luminescent materials was 1 wt.%, DRCs reached the maximum depth. At this time, SMSSED was 5.47 ± 0.18 mm, CAED was 5.00 ± 0.20 mm, and SAED was 4.96 ± 0.04 mm. In addition, compared with CAED and SAED, the composite resin with SMSSED added had a higher curing depth and better curing performance due to the better matching emission wavelength with CQ. Overall, Group A was 9.17 % higher than Group B and 10.27 % higher than Group C.

Table 1. Comparison of curing depth values of three groups of modified composite resins

	Content, wt. %					
	0.00	0.50	1.00	2.00	4.00	6.00
CDA, mm	3.94 ± 0.16	4.47 ± 0.13	5.47 ± 0.18	5.01 ± 0.39	4.88 ± 0.13	4.72 ± 0.14
CDB, mm	3.94 ± 0.16	4.05 ± 0.25	5.00 ± 0.20	4.75 ± 0.05	4.68 ± 0.52	4.54 ± 0.06
CDC, mm	3.94 ± 0.16	4.47 ± 0.13	4.96 ± 0.04	4.84 ± 0.06	4.70 ± 0.08	4.51 ± 0.02

Therefore, the modified dental composite resin prepared by SMSSED has the best performance.

3.2. Effect of SMSSED addition on the related properties of composite resin

To investigate the effect of SMSSED addition on the related properties of composite resin, the modified dental composite resin material is analyzed. Firstly, FTIR and SRD are used to characterize and analyze the modified materials and SMSSED. The FTIR and XRD spectra of composite resin materials doped with different contents of SMSSED are shown in Fig. 4.

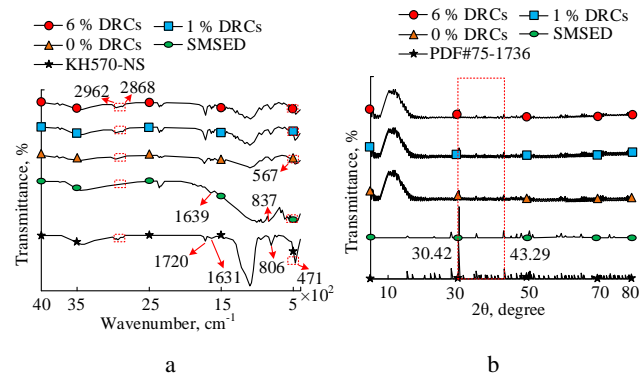


Fig. 4. a–FTIR spectra of SMSSED composite resins doped with different contents; b–XRD patterns of SMSSED composite resins doped with different contents

From Fig. 4 a, the characteristic peaks at 2962 cm⁻¹, 2868 cm⁻¹, and 1720 cm⁻¹ were symmetric and asymmetric stretching vibrations towards -CH₂, as well as stretching vibration absorption peaks of the C=O group. This result confirmed the successful modification of SiO₂ in SMSSED. From Fig. 4 b, the diffraction peaks of DRCs exhibited standard deviation scattering spectra at 30.42° and 43.29°, which were consistent with the standard scattering spectra. This indicates that the incorporation of SMSSED into DRCs is successful.

The double bond conversion rate and mechanical properties of the modified composite resin are shown in Fig. 5. From Fig. 5 a, the double bond conversion rate of all composite resins doped with SMSSED after UV curing was higher than that of composite resins without SMSSED doping. The actual double bond conversion rate of the composite resin doped with 1 wt.% SMSSED was the highest, at 67.29 %. Compared to composite resin without SMSSED doping, the double bond conversion rate increased by 114.16 %. It indicated that SMSSED could significantly improve the curing efficiency of the resin. From Fig 5 b and c, the mechanical properties of the composite resin are improved to a certain extent after doping with SMSSED. On this basis, the fracture surface microstructure of composite resins doped with 0 wt.%, 1 wt.%, 4 wt.%, and 6 wt.% SMSSED is analyzed to verify the effectiveness of SMSSED modification.

The results are shown in Fig. 6.

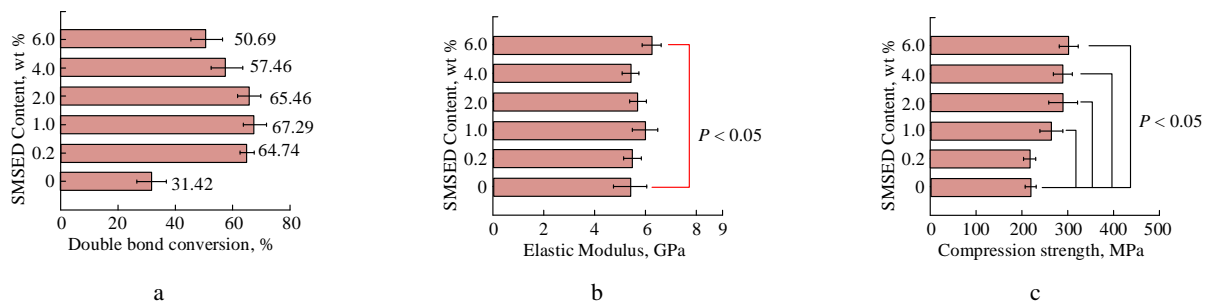


Fig. 5. a–double bond conversion rate of SMSSED composite resin with different doping contents; b–elastic modulus of SMSSED composite resins with different mass ratios; c–compressive strength of SMSSED composite resins with different mass ratios

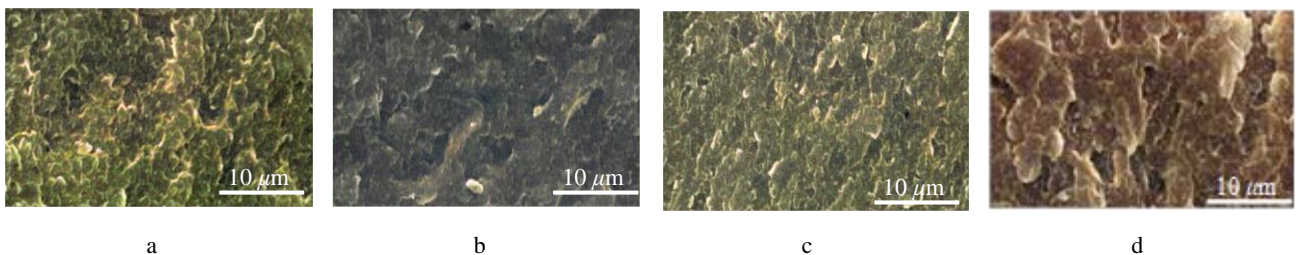


Fig. 6. a–fracture surface morphology of SMSSED composite resin doped with 6 wt.%; b–fracture surface morphology of SMSSED composite resin doped with 4 wt.%; c–fracture surface morphology of SMSSED composite resin doped with 1 wt.%; d–fracture surface morphology of SMSSED composite resin doped with 0 wt.%

From Fig. 6 a, b, and c, compared to Fig. 6 d without SMSED, the fracture surface of the composite resin containing SMSED was more porous and finer. When the SMSED content increased, SMSED couldn't be uniformly distributed in the matrix. SMSED aggregates formed a stress concentration zone, which was prone to cracking. In SMSED composite resin, there was a good bonding force between the matrix and inorganic fillers, without obvious particle aggregation and bubbles. In addition, SMSED was fully covered on the surface of the substrate, demonstrating good interfacial adhesion performance with the substrate.

In addition, the water absorption and solubility results of the modified composite resin are shown in Fig. 7.

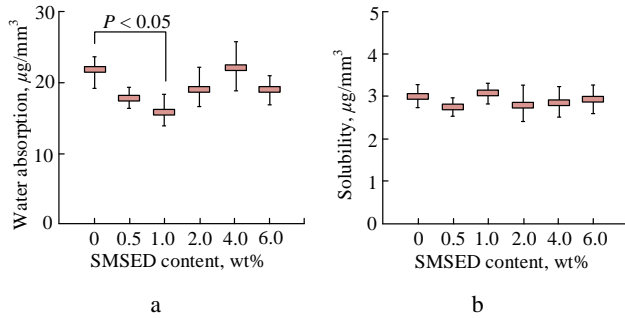


Fig. 7. a–water absorption of SMSED composite resins with different mass ratios; b–solubility of SMSED composite resins with different mass ratios

In Fig. 7 a, the water absorption of the composite resin containing 1 wt.% SMSED was significantly reduced compared to the composite resin without SMSED. Conversely, Fig. 7 b showed no significant change in the solubility of composite resins with varying masses of SMSED, indicating that the structure and size of the composite resin with 1 wt.% SMSED were relatively stable.

The survival rates of L929 cells co-cultured with different concentrations of SMSED composite resin over 1, 2, and 3 days are presented in Table 2. Here, Group 1 represents the survival rate after 1 day, Group 2 after 2 days, and Group 3 after 3 days of cultivation. Additionally, the staining results of live and dead cells with different concentrations of SMSED composite resin are shown in Fig. 8. From Table 2, the composite resin containing 6 % SMSED exhibited the highest cell survival rate at 98.5 ± 10.5 %. Fig. 8 b also showed that the resin with 6 % SMSED maintained a high survival rate of 99.1 ± 3.4 %. Meanwhile, the survival rate for the composite resin with 1 % SMSED was recorded at 95.3 ± 1.2 %. Overall, the experimental results indicated that the survival rates over 1-3 days were consistently above 70 %, demonstrating that the modified composite resin exhibits low toxicity to L929 cells. Fig. 8 further illustrates that actual cell death (indicated in red) for the composite resin with varying

SMSED concentrations was relatively low, suggesting minimal impact on L929 cell viability.

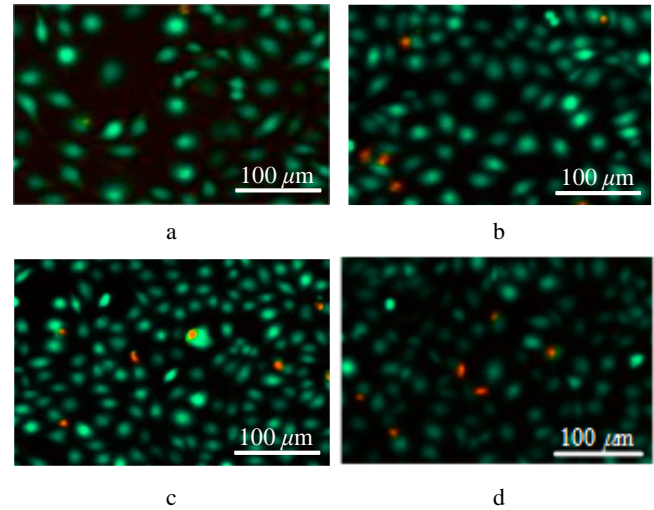


Fig. 8. Staining of live and dead cells using SMSED composite resin with different mass ratios: a–6 % SMSED composite resin; b–4 % SMSED composite resin; c–1 % SMSED composite resin; d–0 % SMSED composite resin

This, combined with the data from Table 2, effectively indicates that the SMSED-modified dental composite resin has low cell toxicity, highlighting its promising application prospects in the oral market.

3.3. Discussion

Group A used $\text{Sr}_2\text{MgSi}_2\text{O}_7$ (usually denoted as SMSED) doped with $\text{Eu}^{2+}/\text{Dy}^{3+}$ as a long afterglow luminescent material for modification of composite resin. Group B used CaAl_2O_4 (usually denoted as CAED) doped with $\text{Eu}^{2+}/\text{Dy}^{3+}$ as a long afterglow luminescent material for modification of composite resin. Group C used $\text{Sr}_4\text{Al}_{14}\text{O}_{25}$ (usually denoted as SAED) doped with $\text{Eu}^{2+}/\text{Dy}^{3+}$ for modification of composite resin. Dy^{3+} $\text{Sr}_4\text{Al}_{14}\text{O}_{25}$ (usually denoted as SAED) is the long afterglow luminescent material for the modification of the composite resin. The main difference between the three groups is the different types of long afterglow luminescent materials used, i.e. SMSED, CAED, and SAED. The filling technique in dental defect repair can avoid further damage. If the caries is significant, crown fracture repair surgery can be used to restore its normal function and appearance [15]. For affected teeth, in clinical practice, the lesion is usually first removed and then filled with appropriate materials, among which DRCs are the most common. Due to its simple construction, beautiful appearance, excellent mechanical properties, low water absorption, and insolubility in water after solidification, DRCs have become the first choice for dental caries.

Table 2. Effect of different concentrations of SMSED composite resin on L929 cell viability

Group	Control	0 wt.%	0.5 wt.%	1 wt.%	2 wt.%	4 wt.%	6 wt.%
1	100	95.0 ± 5.0	91.2 ± 5.8	88.5 ± 8.8	97.3 ± 3.7	93.2 ± 3.8	98.5 ± 10.5
2	100	95.0 ± 3.5	85.5 ± 3.0	86.3 ± 2.7	91.2 ± 2.6	95.4 ± 3.5	99.1 ± 3.4
3	100	95.3 ± 1.2	81.2 ± 0.6	80.0 ± 1.1	91.0 ± 0.3	83.1 ± 0.2	84.0 ± 0.2

Compared with silver amalgam, DRCs have better color matching and higher biological safety [16]. In current research, high content fillers have a negative impact on the conversion of DRCs. It also leads to lower double bond conversion. Therefore, in this study, dental composite resins were modified and prepared using SMSSED to obtain better composite resins for oral gingival fillings. The results showed that the composite resin doped with SMSSED had no other impurity peaks. The $\text{Eu}^{2+}/\text{Dy}^{3+}$ doped CaAl_2O_4 material had a monoclinic crystal structure, while the addition of rare earth ions did not change the crystal structure. After removing the light source, the afterglow is divided into two stages. After radiating SAED powder for 10 minutes and turning off the light source, the intensity of its blue-green afterglow sharply decreased, eventually forming a stable and long-lasting afterglow, which is consistent with the results of others [17].

In addition, when the doping content of SMSSED was 1 wt.%, the double bond conversion rate of DRCs reached 67.29 %, which was 114.16 % higher than that without SMSSED added. When the SMSSED content was 6 wt.%, the increase in double bond conversion rate was the least, but it also increased by 61.33 %. Compared with the results of others, the overall increase in the proposed method is about 10.5 % [18]. Meanwhile, composite resins containing 1 wt.% SMSSED exhibited good structural and dimensional stability. It meets the requirements of the Dentistry-Polymer based-restorative materials (ISO4049) standard. Overall, modifying dental composite resins based on doping SMSSED is effective and practical.

4. CONCLUSIONS

In response to the low monomer conversion rate and insufficient curing depth of DRCs, SMSSED modification is used to prepare dental composite resin. The performance is verified. According to the experimental results, after doping with $\text{Eu}^{2+}/\text{Dy}^{3+}$, CaAl_2O_4 exhibited a monoclinic structure. The addition of rare earth elements had no effect on the crystal structure. Overall, Group A was superior to the control group. The powder of Group A presented a blocky agglomeration state, with a huge size distribution and irregular shape. This result was closer to the relevant particle size distribution of commercial strontium aluminate fluorescent powder, roughly ranging from 10–10 μm . Compared with CAED and SAED, the emission wavelength of SMSSED matches CQ more closely. Therefore, the composite resin with SMSSED added had a higher curing depth and better curing performance, which was 9.17 % higher than Group B and 10.27 % higher than Group C. In addition, the composite resin doped with 1 wt.% SMSSED had the highest actual double bond conversion rate, which was 67.29 %. Compared to composite resin without SMSSED doping, the double bond conversion rate increased by 114.16 %. The fracture surface of composite resin containing SMSSED was looser and finer. The actual dead cells in composite resins doped with different concentrations of SMSSED were relatively low. The biocompatibility test results are encouraging, and the SMSSED modified resin has low toxicity to L929 cells within 1–3 days, with a cell survival rate of over 70 %, indicating that the material has good biocompatibility. In addition, the

water absorption and solubility tests of the modified resin showed that 1 wt.% SMSSED modified resin has lower water absorption and stable solubility. Overall, SMSSED modification for preparing composite resins has practicality and effectiveness. However, the long afterglow material used in the study is still at the micrometer level. Further research is needed to investigate the stable performance of the long afterglow material at the nanometer level. The research improves the mechanical properties and curing efficiency of dental materials using new long afterglow luminescent materials, allowing their materials to maintain good biocompatibility. This is an important advancement for the field of dental surgery, as the materials may lead to better patient outcomes and satisfaction. The study also points to future research into the stability of new materials on nanoscale materials, which may also further advance the science of dental materials.

REFERENCES

1. **Farhadi, E., Omrani, L.R., Estedlal, T., Ahmadi, E.** Deep Margin Elevation with Resin-modified Glass Ionomer in Posterior Adhesive Indirect Restorations Based on Biomimetic Principles: A Case Report *Avicenna Journal of Dental Research* 14 (4) 2022: pp. 190–193. <https://doi.org/10.34172/ajdr.2022.532>
2. **Tran, H.N.M., Nguyen, A.T.D., Tran, T.T.N., Nguyen, K.D., Huynh, N.C.N.** 3D-printed Inlays with Different Cavity Depths Impact Intraoral-scanner's Accuracy In-vitro *MedPharmRes* 7 (4) 2023: pp. 87–94. <https://doi.org/10.32895/UMP.MPR.7.4.11>
3. **Taha, A.I., Hafez, M.E.** An in Vitro Study Measuring Marginal gaps of Inlay Restorations Fabricated from Different CAD-CAM Materials after Thermocycling *BMC Oral Health* 23 (1) 2023: pp. 1–8. <https://doi.org/10.1186/s12903-023-03687-4>
4. **Kang, K.Z., Penukonda, R., Pattar, H., Al-Haddad, A.** Revascularization of an Immature Necrotic Permanent Mandibular Second Premolar with Dens Evaginatus: A Case Report with 3 Years' Follow-up *Endodontology* 34 (4) 2022: pp. 300–305. https://doi.org/10.4103/endo.endo_216_21
5. **Ayari, N., Grira, I., Moussa, A.B.** Cervical Margin Relocation for Indirect Bonded Restorations: A Literature Review *Clinical Medicine and Health Research Journal* 3 (3) 2023: pp. 364–372. <https://doi.org/10.18535/cmhrj.v3i3.167>
6. **López, A.N., Lafebre, M.F., Ramón, M.N.** State of the Art of Biological Thickness in Deep Margin Restorations *World Journal of Advanced Research and Reviews* 18 (3) 2023: pp. 752–759. <https://doi.org/10.30574/wjarr.2023.18.3.1109>
7. **Azim, A.A., Wang, H.H., Serebro, M.** Selective Retreatment and Sinus Lift: An Alternative Approach to Surgically Manage the Palatal Roots of Maxillary Molars *Journal of Endodontics* 47 (4) 2021: pp. 648–657. <https://doi.org/10.1016/j.joen.2020.08.028>
8. **Soliman, S., Casel, C., Krug, R., Krastl, G., Hahn, B.** Influence of Filler Geometry and Viscosity of Composite Luting Materials on Marginal Adhesive Gap Width and Occlusal Surface Height of All-ceramic Partial Crowns *Dental Materials* 38 (4) 2022: pp. 601–612. <https://doi.org/10.1016/j.dental.2021.10.007>
9. **Srivastava, A., Maniakas, A., Myers, J., Chambers, M.S., Cardoso, R.** Reconstruction of Intraoral Oncologic Surgical

Defects with Integra® Bilayer Wound Matrix *Clinical Case Reports* 9 (1) 2021: pp. 213–219.
<https://doi.org/0.1002/ccr3.3501>

10. **Zarif Najafi, H., Estedlal, T., Saki, M., Azmi, A., Mohamadian, F., Moshkelgosh, V.** Er, Cr: YSGG Laser as a Means of Orthodontic Adhesive Removal: Myth or Reality? *Photobiomodulation, Photomedicine, and Laser Surgery* 39 (8) 2021: pp. 558–565.
<https://doi.org/10.1089/photob.2020.4983>
11. **Stacchi, C., Rapani, A., Lombardi, T., Bernardello, F., Nicolin, V., Berton, F.** Does New Bone Formation Vary in Different Sites within the Same Maxillary Sinus after Lateral Augmentation? A Prospective Histomorphometric Study *Clinical Oral Implants Research* 33 (3) 2022: pp. 322–332.
<https://doi.org/10.1111/clr.13891>
12. **Pidgaietskyi, V., Ulianchych, N., Kolomiets, V., Rublenko, M., Andriiets, V.** Osseointegration Properties of Domestic Bioactive Calcium Phosphate Ceramics Doped with Silicon *Polish Journal of Medical Physics and Engineering* 29 (2) 2022: pp. 113–129.
<https://doi.org/10.2478/pjmpe-2023-0013>
13. **Hu, Z., Xu, J., Wang, Y., Xu, L., Yi, Y., Liu, B., Wang, Z.** Efficient Photopolymerization of Dental Resin Composites Using the Photoluminescent Long Afterglow of $\text{Sr}_2\text{MgSi}_2\text{O}_7\text{:Eu}^{2+}, \text{Dy}^{3+}$ *ACS omega* 8 (36) 2023: pp. 32396–32403.
<https://doi.org/10.1021/acsomega.3c01855>
14. **Ismail, H.S., Ali, A.I., Garcia-Godoy, F.** In Vitro Biocompatibility Testing of Different Base Materials Used for Elevation of Proximal Subgingival Margins Using Human Gingival Epithelial Cells *Journal of Oral Science* 64 (2) 2022: pp. 118–123.
<https://doi.org/10.2334/josnusd.21-0393>
15. **Wang, W.J., Grymak, A., Waddell, J.N., Choi, J.J.E.** The Effect of Light Curing Intensity on Bulk-fill Composite Resins: Heat Generation and Chemomechanical Properties *Biomaterial Investigations in Dentistry* 8 (1) 2021: pp. 137–151.
<https://doi.org/10.1080/26415275.2021.1979981>
16. **Braga, S.S.L., Schettini, A.C.T., Carvalho, E.L.O., Shimokawa, C.A.K., Price, R.B., Soares, C.J.** Effect of the Sample Preparation and Light-curing Unit on the Microhardness and Degree of Conversion of Bulk-fill Resin-based Composite Restorations *Operative Dentistry* 47 (2) 2022: pp. 163–172.
<https://doi.org/10.2341/20-043-L>
17. **Ilie, N.** Comparison of Modern Light-curing Hybrid Resin-based Composites to the Tooth Structure: Static and Dynamic Mechanical Parameters *Journal of Biomedical Materials Research Part B: Applied Biomaterials* 110 (9) 2022: pp. 2121–2132.
<https://doi.org/10.1002/jbm.b.35066>
18. **Zhao, Z., Wu, H., Liu, X., Kang, D., Xiao, Z., Lin, Q., Zhang, A.** Synthesis and Characterization of Tung Oil-based UV Curable for Three-dimensional Printing Resins *RSC Advances* 12 (34) 2022: pp. 22119–22130.
<https://doi.org/10.1039/D2RA03182E>



© Zou et al. 2025 Open Access This article is distributed under the terms of the Creative Commons Attribution 4.0 International License (<http://creativecommons.org/licenses/by/4.0/>), which permits unrestricted use, distribution, and reproduction in any medium, provided you give appropriate credit to the original author(s) and the source, provide a link to the Creative Commons license, and indicate if changes were made.